Evolution of sensory systems underlies the emergence of predatory feeding behaviours in nematodes

Marianne Roca[1], Güniz Göze Eren[1], Leonard Böger[1,2], Olena Didenko[1], Wen-sui Lo[3], Monika Scholz[2] & James W. Lightfoot[1*]

1. Max Planck Research Group Genetics of Behavior, Max Planck Institute for Neurobiology of Behavior - caesar, Bonn, Germany.
2. Max Planck Research Group Neural Information Flow, Max Planck Institute for Neurobiology of Behavior – caesar, Ludwig-Erhard-Allee 2, 53175, Bonn, Germany.
3. Northwest A&F University, Yangling, Shaanxi, 712100, China.

* corresponding author

Abstract

Sensory systems are the primary interface between an organism and its environment with changes in selectivity or sensitivity representing key events in behavioural evolution. Here, we explored the molecular modifications influencing sensory perception across the nematode phyla. *Pristionchus pacificus* is a predatory species and has evolved contact-dependent sensing and teeth-like structures to attack prey. Using mutants defective for mechanosensory neuron function, we found an expanded role for this sensory modality in efficient predation alongside its canonical function in sensing aversive touch. To identify the precise mechanism involved in this tactile divergence we generated mutations in 26 canonical mechanosensory genes and tested their function using a combination of behavioural assays, automated behavioural tracking and machine learning. While mechanosensory defects were observed in several mutants, *Ppa-mec-6* mutants specifically also induced predation deficiencies. Previously, a similar phenotype was observed in a chemosensory defective mutant and we found a synergistic influence on predation in mutants lacking both sensory inputs. Importantly, both chemosensory and mechanosensory receptor expression converge on the same environmentally exposed IL2 neurons revealing these as the primary mechanism for sensing prey. Thus, predation evolved through the co-option of both mechanosensory and chemosensory systems which act synergistically to shape the evolution of complex behavioural traits.

Introduction

Sensory systems represent the principal mechanism through which an organism acquires environmental information. These signals can be used for finding food, avoiding predators, detecting mates, and navigating through complex surroundings (Stevens, 2013). Detecting these environmental cues is dependent on specialised sensory systems which are often finely tuned to specific stimuli. Crucially, these systems are not static and their modification can profoundly affect the evolutionary trajectory of a species. Mechanisms of sensory system evolution include modifications to receptors such as changes to receptor selectivity or sensitivity as well as associated gene losses or gains (Oteiza and Baldwin, 2021). Examples of such events have been observed in several invertebrate species with changes in receptor function influencing feeding ecology in fruit flies (Auer et al., 2020; Prieto-Godino et al., 2017), mosquitoes (McBride et al., 2014), and cockroaches (Wada-Katsumata et al., 2013). Similarly, in vertebrates, changes to sweet receptors have modified the feeding behaviours of songbirds and bats (Hall et al., 2021; Jiao et al., 2021; Toda et al., 2021) while in deep sea fish, a greatly expanded number of opsins has evolved to maximise their visual sensitivity in minimal light environments (Musilova et al., 2019). Thus, sensory system evolution shapes the behavioural repertoire of an organism and facilitates its adaptation to its ecological niche.

In nematodes, a remarkable range of behaviours has evolved in accordance with the diverse ecologies found across the phyla. In particular, with their exceptional array of genetic and molecular tools (Eren et al., 2022; Han et al., 2020; Rödelsperger et al., 2017; Witte et al., 2015) alongside their distinct feeding ecologies, *Caenorhabditis elegans* and *Pristionchus pacificus* represent a powerful interspecies system for understanding the evolutionary adaptations influencing sensory perception. More specifically, while *C. elegans* is a microbial feeder, *P. pacificus* is an omnivorous species and not only feeds on bacteria but is also a predator of other nematodes (Wilecki et al., 2015). This expanded feeding behaviour is linked to a mouth-form plasticity with *P. pacificus* nematodes capable of developing one of two morphs (Bento et al., 2010; Ragsdale et al., 2013). These are either the stenotomatous (st) or eurystomatous (eu) form. The st mouth is narrow with a single tooth and only permits bacterial feeding or scavenging whereas the eu mouth is wider and possess an additional tooth which facilitates both bacterial feeding and predation (Wilecki et al., 2015). Furthermore, predation behaviour is directed towards not only other nematode species but also con-specifics. However, closely related strains are spared due to the presence of a robust kin recognition system (Lightfoot et al., 2019; Lightfoot et al., 2021). Crucially, how sensory systems evolved to accommodate the predatory behaviours is an open question.

In *C. elegans*, bacterial food is detected through well described foraging behaviour using their chemosensory and texture sensing systems (Bargmann, 2006; Tanimoto et al., 2016; Zjacic and Scholz, 2022). In *P. pacificus*, little is known of its food and prey sensing mechanisms, however, they show specific

sensory adaptations relevant to their ecology. In particular, *P. pacificus* are attracted to many bacterial species found concurrently in their environment and are also attracted to specific insect pheromones as *Pristionchus* are frequently found associated with scarab beetles (Akduman et al., 2018; Hong and Sommer, 2006; Hong et al., 2008). During food sensing and foraging, *P. pacificus* transitions between the docile bacterial feeding and aggressive predatory feeding states through the internal balance of octopamine and tyramine. These neuromodulators act on a group of head sensory neurons expressing the corresponding receptors (Eren et al., 2024). Contact between the nose of the predator and the surface of the prey during aggressive predatory bouts can initiate the activity of their movable tooth to puncture through the cuticle of the prey (Ishita et al., 2021; Moreno et al., 2019; Okumura et al., 2017; Wilecki et al., 2015). However, the precise stimuli responsible for detecting prey contacts are currently unknown.

Here, to understand how the *P. pacificus* sensory systems have contributed to the emergence of predatory feeding we have investigated the role of mechanosensory adaptations for these behaviours. Using a candidate-based approach, we identified a crucial role for mechanosensation in predation. We find *Ppa-mec-6* is necessary for this process and may contribute to these behaviours through a previously undescribed predatory-associated mechanosensory channel. Furthermore, we demonstrate that mechanosensation is required alongside chemosensory inputs and that these acts synergistically for efficient predation behaviours. Finally, we also reveal chemosensory and mechanosensory components are expressed in the same externally projecting and environmentally exposed neurons indicating functional convergence into the same sensory circuits.

Results

Mechanosensation is involved in prey detection

P. pacificus is a voracious predator of other nematode larvae including *C. elegans* and this feeding behaviour requires contact between predator and prey (Fig. 1A). Accordingly, we investigated the importance of *P. pacificus* mechanosensation for detecting prey and how these abilities may have emerged to facilitate the evolution of its predation behaviours. *Cel-mec-3* is critical transcription factor involved in the development and function of mechanosensory neurons in *C. elegans,* and mutants in this gene fail to respond to tactile stimuli (Chalfie and Sulston, 1981; Way and Chalfie, 1988). In *P. pacificus,* using a *Ppa-mec-3* transcriptional reported we also observed its expression in several neurons with similar cell body placements to the *C. elegans* mechanosensory neurons FLP, AVM, ALM, PVM, PVD, and PLM (Fig. 1B), (Liska et al., 2023; Singh et al., 2024). To assess its role in mechanosensation, we generated a mutation in the *Ppa-mec-3* orthologue using CRISPR/Cas9. Similar to *C. elegans*, we found *Ppa-mec-3* mutants fail to react to several classic mechanosensory assays including harsh touch, gentle touch, and nose touch assays (Fig. 1C-E). Taken together, this indicates a conserved role for *Ppa-mec-3* between species. Next, to assess

a potential role for *Ppa-mec-3* in predatory feeding, we performed previously established corpse assays (Wilecki et al., 2015). In corpses assay, starved *P. pacificus* adults are placed in a plate full of *C. elegans* larvae and predation success is determine by the number of corpses after a designated time interval (supplementary Fig. 1A). Here, *Ppa-mec-3* show a significant reduction in killing ability with fewer larval corpses generated by predators than observed by wildtype animals (Fig 1F). Thus, mechanosensory systems have acquired additional functions in *P. pacificus* and are also necessary for efficient prey detection.

Mechanosensory genes have diversified across evolution

Having established the importance of mechanosensation for predation, we next explored the conservation of mechanosensory gene networks across nematode evolution. Frequent gene losses and gains are observed between nematode species and this can be associated with evolutionary novel processes (Blaxter, 2011; Prabh et al., 2018). Therefore, we initially conducted a bioinformatic study of the mechanosensory systems across 8 nematode species to investigate the evolution of this sensory modality across the nematode phyla (Fig. 2A). Our analysis consisted of the two free-living species *C. elegans* and *P. pacificus* belonging to clade 5 as well as several obligate parasite species of both plants and animals (Blaxter, 2011). We focused mostly on orthologues of the *C. elegans* predicted mechanostransduction channels belonging to the degenerin–epithelial Na+ channels (DEG/ENaC), and transient receptor potential (TRP) gene families (Goodman, 2006) as well as other known mechanosensory genes including *mec-6*, a paraoxonase-like protein which acts as a chaperone to ensure channel function (Chen et al., 2016), and *pezo-1*, due to its reported role in food sensation (Millet et al., 2022). Compared to free-living nematodes, parasitic nematodes frequently had a lower number of genes encoding for mechanotransduction channels perhaps indicative of adaptations to their specific lifestyle. In contrast, comparisons between the free-living nematodes *C. elegans* and *P. pacificus* generally showed a similar representation of gene families with a few exceptions (Fig. 2A). These include the four *trpl* genes which are specific to *C. elegans* and are absent in other species including *P. pacificus* (Goodman, 2006). Additionally, there are two large gene expansions in *P. pacificus* among the DEG/ENaC gene family with five copies of *deg-1* in *P. pacificus* compared to one in *C. elegans* and 11 *egas* genes in *P. pacificus* compared to four in *C. elegans*. Little is known regarding the function of *egas* in *C. elegans* and many of the *P. pacificus egas* paralogues lack RNA-seq data to validate their expression (Athanasouli et al., 2020; Rödelsperger et al., 2017). However, *deg-1* has been shown in *C. elegans* to be required for the induction of mechanoreceptor current in the sensory ASH neuron (Geffeney et al., 2011). Therefore, mechanosensory gene networks appear relatively stable between *C. elegans* and *P. pacificus* but are more stochastic in parasitic nematodes with their more complex life-styles and host interactions.

With the identification of genes potentially acting as mechanosensory channels in *P. pacificus,* we conducted a candidate-based approach to identify potential components necessary for efficient prey detection through *P. pacificus* nose contact. Candidates were selected based on known mechanosensory phenotypes in *C. elegans* together with further validation through available *P. pacificus* expression data (Athanasouli et al., 2020; Baskaran et al., 2015; Rödelsperger et al., 2017). Accordingly, we selected genes to target by CRISPR/Cas9 which included both TRP and DEG/ENaC families as well as other associated mechanosensory genes. We selected the DEG/ENaC channels *Ppa-mec-4* and *Ppa-mec-10* as well as *Ppa-mec-6*. In *C. elegans, Cel-mec-4* and *Cel-mec-10* are both involved in the gentle touch response (Bianchi, 2007; Chalfie and Sulston, 1981; Staum et al., 2024) and *Cel-mec-6* has been shown to directly interact with *Cel-mec-4* and *Cel-mec-10* to aid the function and stability of this mechanosensitive channel (Chelur et al., 2002; Chen et al., 2016). We targeted *Ppa-osm-9, Ppa-ocr-2* and *Ppa-trp-4* together as in *C. elegans* these genes have an additive effect reducing its nose touch responsiveness (Chatzigeorgiou et al., 2010). Only *P. pacificus* triple mutants for these genes were analysed. *C. elegans* nose touch response also requires *Cel-delm-1* and *Cel-delm-2* which are expressed in glial cells (Han et al., 2013). However, we could not identify one to one orthologue of these two genes in *P. pacificus* as both paralogous sequences are closer to each other than to *Cel-delm* or *Cel-acd* genes. Therefore, these were named *delm/acd* and we targeted both candidates in *P. pacificus*. In *C. elegans, Cel-del-7* and *Cel-del-8* are DEG/ENaC ion channel family members with the first involved in mechanotransduction (Rhoades et al., 2019), however, there is only one paralogue in *P. pacificus* which we also targeted and named *Ppa-del-7/8*. We also generated a quintuple mutant targeting all paralogues of DEG/ENaC *Ppa-deg-1* and targeted the DEG/ENaC potential proprioception genes *Ppa-del-1, Ppa-unc-8* and *Ppa-unc-105* (Bianchi, 2007; Tao et al., 2019). To further represent the TRP gene family, we included *Ppa-trp-1, Ppa-trp-2, Ppa-pkd-2, Ppa-cup-5* and *Ppa-trpa-1* which in *C. elegans* are expressed in many neurons and most have roles in mechanotransduction (Chatzigeorgiou et al., 2010; Han et al., 2013; Kindt et al., 2007; Xiao and Xu, 2009). Finally, we target the ionotropic glutamate receptor *Ppa-glr-1* due to its role in mediating excitatory neurotransmission in touch receptor neurons (Hart et al., 1995) and *Ppa-pezo-1* due to potential roles in food sensing (Millet et al., 2022). This resulted in 26 genes of interest and we investigated two alleles for each of these genes which were predicted to cause loss of function mutations (Supplementary Table 1).

MEC-6 is required for efficient *P. pacificus* predation

Initially, we tested all of our mutants for mechanosensory defects using the three touch assays adapted from previous *C. elegans* studies. These were assays measuring the animal response to harsh touch, gentle touch, and nose touch (Chalfie et al., 2014). The majority of the *P. pacificus* mutants did not show mechanosensory deficient phenotypes. However, *Ppa-mec-4, Ppa-mec-10,* and *Ppa-mec-6* showed

mechanosensory defects similar to those described in *C. elegans* and also similar to those observed in *Ppa-mec-3* resulting in a response to touch only half the time or less (Fig. 2B-D and supplementary Fig. 1B-D). Furthermore, all four mutants were also more lethargic than wildtype worms which also phenocopies *C. elegans* mechanosensory mutants (Staum et al., 2024). Thus, as in *C. elegans, Ppa-mec-4, Ppa-mec-10, Ppa-mec-3* and *Ppa-mec-6* are required for touch sensation in *P. pacificus*. While previous reports in *C. elegans* have not identified a role for harsh touch sensation in *Cel-mec-4* (Chatzigeorgiou et al., 2010), this discrepancy between the two species may stem from subtle species specific sensitivity differences. Next, we tested all of our mutants for defects in predation using the previously described corpse assays. While the majority of mutants displayed wildtype levels of predation, a reduced level of killing was observed in *Ppa-mec-6* (Fig 2E and supplementary Fig. 1E). This is similar to the defect observed in the *Ppa-mec-3* mutants (Fig. 1F). Importantly, no predatory defect was observed in *Ppa-mec-4* or *Ppa-mec-10* indicating the predatory abnormality is not dependent on the mechanosensation deficient phenotype in general but is specific to the function of *Ppa-mec-3* and *Ppa-mec-6.* In *C. elegans, Cel-mec-6* is involved in the assembly and function of mechanosensory ion channels and interacts with *Cel-mec-4* and *Cel-mec-10* to form ion channel complexes that are essential for mechanotransduction (Brown et al., 2008). Our data indicates that the *Ppa-mec-4* and *Ppa-mec-10* channel is not required for prey detection in *P. pacificus* and instead suggests *Ppa-mec-6* may act in an additional as yet unknown mechanosensory ion channel involved in determining prey contact. Thus, specific mechanosensory inputs are necessary for prey detection in *P. pacificus.* However, as predation is not fully abolished, additional sensory inputs also contribute to its prey detection abilities.

Mechanosensation and other predatory associated traits

Predation in *P. pacificus* is dependent on the formation of the eu mouth morph which is determined by a multitude of environmental and genetic factors (Casasa et al., 2023; Dardiry et al., 2023; Ragsdale et al., 2013; Sieriebriennikov et al., 2020; Werner et al., 2017; Werner et al., 2023). To assess if mechanosensation also influences the mouth morph fate, we screened our mutant library for any effect on mouth form ratio. All mutants showed wildtype levels of eu to st morphs (supplementary Fig. 2A and B). In addition, *P. pacificus* has a robust kin-recognition mechanism which prevents attacks on its own progeny and close relatives while facilitating the cannibalism of other con-specific competitors (Lightfoot 2019, 2021). Due to the prey detection defect observed in *Ppa-mec-3* and *Ppa-mec-6* we also tested these mutants for kin-recognition defects. For both *Ppa-mec-3* and *Ppa-mec-6* mutants, kin-recognition was robustly maintained indicating no deficiency in this process (supplementary Fig. 2C). Therefore, defects in mechanosensation are specific to prey detection and do not influence other predatory traits.

Chemosensation and mechanosensation synergistically influence prey detection

The partial defect in prey detection observed in the *Ppa-mec-3* and *Ppa-mec-6* mutants are similar to those previously describe in cilia deficient mutants (Moreno et al., 2019). Cilia are complex organelles and in nematodes they are essential for the detection of many environmental cues. In both *C. elegans* and *P. pacificus* some of the strongest cilia deficiencies are observed in mutants defective for the transcription factor *daf-19* which acts as the master regulator of ciliogenesis (De Stasio et al., 2018; Moreno et al., 2018; Moreno et al., 2019). Curiously, while mutations in *Cel-daf-19* show aberrant dauer entry, in *P. pacificus* no dauer abnormal phenotypes are observed in *Ppa-daf-19* reinforcing the distinct evolutionary trajectories regulating this developmental process between these species (Lo et al., 2022). Furthermore, accompanying the numerous chemosensory defects in *Ppa-daf-19*, these mutants are also defective in prey detection (Moreno et al., 2019). Therefore, to disentangle the roles of chemosensation and mechanosensation we assessed the *Ppa-mec-3* and *Ppa-mec-6* mutants alongside *Ppa-daf-19.* We found that while *Ppa-daf-19* mutants showed chemosensory defects in their attraction to a bacterial food source and in their aversion to octanol, both *Ppa-mec-3* and *Ppa-mec-6* responded as wildtype animals to these cues (Fig. 3 A and B). This indicates both *Ppa-mec-3* and *Ppa-mec-6* are not defective for chemosensation. In contrast, while both *Ppa-mec-3* and *Ppa-mec-6* are mechanosensory defective, the touch response of *Ppa-daf-19* mutants was similar to wild type animals (supplementary Fig. 2 B-D). A similar observation has also been reported in *C. elegans* where only mild mechanosensory defects are observed in *Cel-daf-19* mutants (Perkins et al., 1986). Thus, mechanosensory defects appear specific to *Ppa-mec-3* and *Ppa-mec-6* while *Ppa-daf*-19 mutants are mostly associated with chemosensory defects. As both groups of mutants are defective for prey detection but neither fully abrogates the *P. pacificus* predatory abilities, we next assessed if these sensory inputs act synergistically. Double mutants of *Ppa-mec-6; Ppa-daf-19* and triple mutant either *Ppa-mec-3; Ppa-mec-6; Ppa-daf-19* exacerbated the predation defect further, however, crucially some killing was still maintained (Fig. 3C). Therefore, chemosensation and mechanosensation act in parallel for prey detection. Remaining killing abilities may act through some residual function in these sensory pathways or through another as yet unidentified stimuli.

Behavioural tracking and state predictions

Quantifying the number of *C. elegans* corpses generated by *P. pacificus* predators provides a robust assessment of overall killing ability (Wilecki et al., 2015). However, understanding the sensory-motor transformations underpinning a prey contact require more detailed behavioural analyses. We recently developed an automated behavioural tracking and machine learning model to identify and quantify aggressive behavioural states associated with predation and further analyse these complex behaviours (Bonnard et al., 2022; Eren et al., 2024). Using this method, the *P. pacificus* behavioural repertoire can be

divided into six states. These consist of three predatory associated states including 'predatory search', 'predatory biting' and 'predatory feeding' (Fig. 4A). Additionally, three non-predatory behaviours including a 'dwelling' state and two 'roaming' states exist which are similar to behavioural states observed in *C. elegans* (Eren et al., 2024; Flavell et al., 2013). The two most predictive features of predation states are velocity and pumping rate. By observing the joint distribution of these two features, it is possible to visualize the prevalence of predatory and non-predatory states (Fig. 4A). We use a machine learning models that was previously trained on behavioural data using both unsupervised and supervised methods (Eren et al., 2024) to investigate behavioural state occupancy in our predation mutants compared to wildtype animals (Fig. 4 and supplementary Fig. 3). In the mechanosensory defective *Ppa-mec-6* and *Ppa-mec-3* as well as the chemosensory defective *Ppa-daf-19* mutants, we found a significantly increased in the duration and total time spent into the 'predatory search' state. This may be indicative of a compensatory mechanism whereby the loss of one sense enhances utilisation of the remaining senses. This is further supported by the absence of this phenotype in mutants lacking both sensory modalities including the double mutants *Ppa-mec-6; Ppa-daf-19* and *Ppa-mec-3; Ppa-daf-19* as well as a significant decrease in the triple mutant *Ppa-mec-3; Ppa-mec-6; Ppa-daf-19*. Instead, in these mutants we find a significant increase in the non-predatory 'search' and 'roaming' states indicating a switch away from predatory states and into exploratory behaviours. This is similar to observations in *C. elegans* where the loss of one or multiple sensory modalities results in modifications to the performance of the remaining senses and induces behavioural adjustments (Rabinowitch et al., 2016; Staum et al., 2024). Furthermore, 'predatory biting' state occupancy was similar to wildtype animals in both *Ppa-mec-6* and *Ppa-mec-3* mutants while, in *Ppa-daf-19* this state was significantly reduced. Therefore, predatory behavioural states are modulated through signals received through the *P. pacificus* sensory systems with both chemosensory and mechanosensory modalities influencing distinct but overlapping aspects of prey detection.

Prey detection systems converge on the IL2 sensory neurons

Finally, as distinct mechanosensory and chemosensory inputs contribute to the *P. pacificus* predatory abilities, we investigated if they act through discrete independent neurons or if instead, they converge into the same sensory pathways. To resolve this, we generated a reporter strain expressing *Ppa-mec-6p*::Venus and *Ppa-daf-19p*::RFP and identified the specific prey detection neurons involved. We observed *Ppa-mec-6* expression in the putative *P. pacificus* ALM and PLM body neurons. Additionally, *Ppa-mec-6p*::Venus and *Ppa-daf-19p*::RFP co-localised and were robustly expressed in the *P. pacificus* IL2 neurons (Fig. 5A and B). These were identified based on soma position and their unique morphological features (Cook et al., 2024). Importantly, the anterior processes from this group of six neurons project into the external environment through exposed sensory endings making them strong candidates for prey

detection (Fig. 5C). As in *C. elegans*, many sensory neurons in *P. pacificus* are ciliated and this is not restricted to the IL2 sensory neurons (Moreno et al., 2018). Therefore, it is somewhat surprising that the most robust *Ppa-daf-19* expression is observed in the IL2 neuron cluster. However, as there are several large introns in the *Ppa-daf-19* gene structure which contain enhancers and other epigenetic signatures (Werner et al., 2018), we predict these may contribute additional regulatory elements for further expression in other ciliated neurons. These may currently be missing from our *Ppa-daf-19p*::RFP reporter. Thus, both mechanosensory and chemosensory prey detection systems converge on the same head neurons with sensory projections exposed to the external environment and which act as the first point of contact with potential prey.

Discussion

A central aspect associated with the evolution of predatory behaviours hinge on an organism's capability to detect potential prey. Fundamental to this are adaptations to sensory abilities that enable an organism to perceive, process and respond to potential prey cues and direct predatory behaviours appropriately. In the nematode *P. pacificus*, we have found that the evolution of predation is associated with the diversification and specialisation of both mechanosensory and chemosensory modalities to also encompass prey detection (Fig. 5D). This is beyond there previously described function in the model species *C. elegans*. The co-option and neofunctionalisation of sensory systems are frequently observed phenomenon. For example, the lateral line system, used to detect water movements and vibrations in many fish species, has evolved electroreception capabilities in sharks, rays and skates (Bellono et al., 2017; Kalmijn, 1971; Kalmijn, 1982; Murray, 1960). Similarly, certain snake species including pit vipers, pythons and some boas have evolved infra-red detection through adaptations to the temperature-sensitive skin thermotransduction receptor TRPA1. This enables these species to hunt warm blooded prey in near total darkness while in other snakes it is a mechanism to regulate body temperature (Gracheva et al., 2010; Krochmal et al., 2004). Examples of sensory co-option events are not restricted to animals and can also be readily found in plants including carnivorous Venus flytrap and sundew species whereby ancestral mechanosensory channels are instead used for sensing and prey capture (Procko et al., 2021; Procko et al., 2023). Therefore, our findings support a well-established link between sensory system evolution and behavioural diversity across a wide range of taxa.

In *P. pacificus*, the co-option and integration of multiple sensory modalities, suggests that predation is not solely dependent on enhancements and adaptations to a single sensory pathway but rather on the evolution of multiple interacting systems which fine tune prey capture. In this nematode species, it is both chemosensation and mechanosensation that are required for efficient predation. Similar multimodal mechanisms of predation can be observed in other invertebrates, including other species which also lack

visual inputs or those which hunt in low light environments. These include species of octopus which utilise chemotactile receptors on their tentacles to identify potential prey through a mechanism of contact-dependent aquatic chemosensation (van Giesen et al., 2020). Additionally, cone snails are carnivorous molluscs that hunt fish, worms or other snails using chemosensation to firstly detect the presence of chemicals secreted by their prey and subsequently vibration sensing and mechanoreception to determine prey position. They then shoot a venomous harpoon-like tooth to immediately immobilise and feed on their target (Dutertre et al., 2014; Olivera et al., 2015; Salisbury et al., 2010). In *P. pacificus*, our data shows that both chemosensation and mechanosensation are important for predation and defects in either system significantly reduce killing ability. Additionally, from our behavioural state studies of these mutants, we find defects in *Ppa-daf-19* chemosensory mutants are more severe and are associated with both aberrations in 'predatory biting' states alongside increased 'predatory search' occupancy. A similar 'predatory search' occupancy increase is also detected in *Ppa-mec-3* and *Ppa-mec-6* mutants. We hypothesis the increased 'predatory search' state occupancy in both sensory modalities is a compensatory mechanism whereby *P. pacificus* switches dependency to the unimpaired sense in an attempt to maintain its predatory behaviours. This is further validated by the loss of this increase in mutants lacking both the predatory associated mechanosensory and chemosensory components. Indeed, sensory loss in *C. elegans* has also been shown to alter the performance of remaining sensory modalities resulting in distinct behaviours (Rabinowitch et al 2016, Staum et al 2024). Furthermore, while the mechanosensory *Ppa-mec-6* and *Ppa-mec-3* as well as chemosensory *Ppa-daf-19* mutants show reduced killing abilities, *Ppa-mec-6* and *Ppa-mec-3* mutants were found to occupy 'predatory biting' states similar to wildtype while this state was reduced in *Ppa-daf-19*. Therefore, both sensory inputs likely have specific functions during predation with chemosensation potentially required throughout these behaviours while mechanosensory systems may be associated with the initial steps of the predator-prey contact.

Both *daf-19* and *mec*-3 are transcription factors and influence genes associated mostly with chemosensation and mechanosensation respectively (Moreno et al., 2018; Way and Chalfie, 1988). This makes it difficult to disentangle the precise molecular mechanisms associated with the emergence of the predatory behaviour in *P. pacificus* using these mutants alone. However, by focusing on the role of mechanosensation, we have been able to identify *Ppa-mec-6* as a specific molecular component that has acquired additional functions in *P. pacificus* associated with its predatory feeding. In *C. elegans*, *Cel-mec-6* is a known to interact with several DEG/EnAC type subunits with the best characterised being *Cel-mec-4* and *Cel-mec-10* which form a mechanosensory ion channel responsible for the gentle touch response (Chalfie and Wolinsky, 1990; Chelur et al., 2002; Chen et al., 2016; Shreffler et al., 1995). Within this complex *Cel-mec-6* is a small auxiliary protein that is not a pore-forming subunit itself but is necessary for proper channel function. In *P. pacificus*, we find mutations in any of *Ppa-mec-4*, *Ppa-mec-10* or *Ppa-mec-*

6 result in mechanosensory defects but it is only *Ppa-mec-6* that has additional predation-specific abnormalities. Thus, while *Ppa-mec-6* may interact with *Ppa-mec-4* and *Ppa-mec-10* to regulate mechanosensation as in *C. elegans*, it is also likely involved with other as yet unknown components and may form a distinct mechanosensory channel involved in prey detection. These components require further identification.

By analysing the localization of *Ppa-mec-6*, we observed robust expression in the six head sensory IL2 neurons where it is also expressed in *C. elegans*(Hammarlund et al., 2018) . These neurons are easily identified in *P. pacificus* by their morphology and soma location which also show a distinct placement compared to *C. elegans* (Cook et al., 2024; Cros and Hobert, 2022). In both species, the IL2 neurons project neurites toward the nematode nose with the sensory endings exposed to the external environment. In *C. elegans*, these neurons regulate dauer formation and nictation behaviours and are thought to be both chemosensory and mechanosensory (Androwski et al., 2020; Lee et al., 2011; Schroeder et al., 2013). Crucially, recent studies in *P. pacificus* identified the IL2 neurons as regulators of predatory feeding states which depend on the balancing actions of octopamine and tyramine (Eren et al., 2024). Octopamine induces predatory states while tyramine initiates more docile bouts and IL2 neurons express octopamine receptors necessary for the predatory states in *P. pacificus*. Accordingly, our findings that these neurons express *Ppa-mec-6* as well as *Ppa-daf-19* reinforces their importance as prime candidates for detecting and determining prey contact events. Moreover, the convergence of both mechanosensory and chemosensory inputs as well as behavioural state modulatory mechanisms in the *P. pacificus* IL2 neurons demonstrates that even relatively simple circuits can be remodelled to accommodate complex and dynamic behaviours including predation. Therefore, taken together, our findings provide new insights into how sensory systems are co-opted and refined to generate behavioural diversity, and demonstrate the importance of sensory perception and evolutionary adaptations for establishing novel behavioural traits.

Materials and methods

Worm maintenance

Worms, *P. pacificus* (PS312 and derived strains) or *C. elegans* (N2), were maintained on nematodes growth media (NGM) 6 cm plates seeded with 300 µl *Escherichia coli* (OP50) at 20ºC. All *P. pacificus* strains used are listed in supplementary table 1. The *C. elegans* N2 strain was provided by the CGC, which is funded by NIH Office of Research Infrastructure Programs (P40 OD010440).

Orthologue identification

We retrieved mechanotransduction channel list from wormBook (Goodman, 2006) and obtained published genome assemblies for eight nematode species belonging to different clades identified by Blaxter

et al (Blaxter et al., 1998). These species include: *Pristionchus pacificus* (Rödelsperger et al., 2017), *Caenorhabditis elegans* (release WS271, 2019, WormBase website (Sternberg et al., 2024)), *Strongyloides ratti* (Hunt et al., 2016), *Bursaphelenchus xylophilus* (Dayi et al., 2020), *Brugia malayi* (Choi et al., 2011; Foster et al., 2005), *Ascaris suum* (Wang et al., 2008), *Romanomermis culicivorax* (Schiffer et al., 2013) and *Trichinella spiralis* (Korhonen et al., 2016). When multiple annotated isoforms were available, only one was considered for analysis. Orthologous were determined using OrthoFinder (Emms and Kelly, 2019).

Generation of new strains

Mutations were induced by CRISPR/Cas9 (IDT) by co-injection of the gRNA for the gene of interest while using a gRNA targeting *prl-1* as a marker as previously described (Nakayama et al., 2020). gRNAs were made by mixing crRNA (IDT) and tracrRNA (IDT) in equal volume and quantity and incubated for 5 min at 95ºC. After letting them cooldown 5 min at room temperature, up to three gRNA were mixed with the Cas9 and 5 min later Tris-EDTA (TE, Promega) was supplemented to reach the concentration of 18.1 µM for sgRNA and 12.5 µM for Cas9. This mix was centrifuged for 10 min at maximum speed at 4ºC. The resulting mix was used to inject *P. pacificus* adults in the gonads area (Axiovert 200, zeiss and Eppendorf set up). P0 injected worms were singled out and laid eggs overnight. Once the progeny had developed enough, plates were screened for a roller phenotype induced by the dominant mutation in *prl-1* pointing to successful injection. Around 50 worms were genotype from identified plates for the gene of interest using PCR (Qiagen) followed by sanger sequencing (Eurofins). The gRNA and primer sequences used as well as the wild-type sequences and generated mutation are provided in supplementary table 2. Two guide RNA were used for *mec-3* to target both isoforms. All mutations generated are predicted to lead to an early stop codon or frameshift with the exception of one allele of *Ppa-mec-3 (bnn61)* and one allele of *Ppa-trp-2 (bnn51*) presented in supplementary figures. Mutations were generated in the *P. pacificus* PS312 strain. Mutations primers and gRNA sequences can be found in Supplementary table 2)

Behavioural tracking and state predictions required an integrated *myo-2p*::RFP (Eren et al., 2024). In addition, mouth morph ratio is influenced by *Ppa-daf-19* which results in a strong St bias unsuitable for predation assays (Moreno et al., 2019). Therefore, predatory morphs Eu were induced alongside *Ppa-daf-19* through generation of additional mutations in *Ppa-nag-1; Ppa-nag-2* (Sieriebriennikov et al., 2018) in the *myo-2p*::RFP background. Accordingly, this strain JWL118 has a 100% Eu mouth morphs (Supplementary Fig. 3A). For experiments involving *Ppa-daf-19*, all comparative experimental strains also carry *Ppa-nag-1; Ppa-nag-2* mutations based on the control strain JWL147 (see supplementary table 1).

Generation of reporter lines

TurboRFP and GFP sequences optimized for *P. pacificus* were retrieved from plasmid pZH009 and pZH008 respectively (Han et al., 2020). A Venus reporter (Nagai et al., 2002) was optimised for *P. pacificus* as previously described (Han et al., 2020). Promotor sequences consisted of the indicated number of nucleotides preceding the ATG according to *P. pacificus* genome (Rödelsperger et al., 2017) *Ppa-mec-6* (949 bp), *Ppa-mec-3* (932 bp), *Ppa-daf-19* (719 bp) promotor sequences. *daf-19p*::RFP (pMR027, Genscript) and *mec-6p*::Venus (pMR022, eurofins) were made by gene synthesis. For generating stable transgenic lines, animals were injected with a mix containing 60 ng/ µl purified gDNA (NEB Monarch purification kit) along with 5- 10 ng/µl plasmid of interest all digested with HindIII. Prior to each injection, the mix was centrifuged at maximum speed at 4ºC for 10 min. Injection were made in *P. pacificus* adult gonads (Axiovert 200, zeiss, and Eppendorf set up). Progeny worms carrying the construct of interest were identified using the epi-fluorescence microscope (Axio Zoom V16; Zeiss). Confocal images were acquired using a stellaris microscope (Leica) with a 63x objective at water immersion.

Chemosensory assays

Attraction toward OP50 was tested using previously developed assays with minor modifications (Moreno et al., 2018). 20 µl of an OP50 overnight culture was pipetted onto a 6 cm unseeded plate 1.5 cm from the edge and left at room temperature overnight. Plates where then kept in the fridge until use. 50 adult worms from plates almost depleted of food were placed at the opposite side of the bacterial lawn at around 1.5 cm of the border making sure to not transfer any bacteria when doing so. After 8 hours the number of worms at the bacterial lawn and the total number of worms still alive in the plates were determined. Plates were scored if they had at least 30 worms left at the end of the assay.

To assess worm behaviour toward 1-octanol, we adapted existing protocols (Lo et al., 2022). Adult worms were washed off with M9 and left on an unseeded plate for 3 hours to remove bacteria. Prior to starting the assay, two drop of 1.2 µl of sodium azide 1M was deposit 3 cm apart on opposite side of a 6 cm unseeded plate. 100 worms were placed in the middle line between the two drops and immediately 1µL of 100% ethanol was put as control on top of one of the sodium azide deposits and 1 µl of 100% 1-octanol (sigma-aldrich) over the other. The assay plates were left for 16 hours at 20°C before assessing worm position. Only worms within a 2 cm radius of the drop up to the midline were taking into account and plates with at least 40 worms at the end of the assay. Chemosensation index was calculated as the ratio between the number of worm closer to the 1-octanol minus those closer to the ethanol relative to the total number of worms. For both assays 10 replica were made over at least three different days.

Touch assays

Touch assays were performed as described for *C. elegans* with minor modifications (Chalfie et al., 2014). Worms were transferred to unseeded plates and left to recover for several minutes prior to being utilised in one of the three assays. Harsh touch assays consisted of touching the worm between its vulva and its tails with the platinum pick used in every day worm maintenance. For the gentle touch assays, the worm was caressed with an eyelash (taped to a wood skewer pick for handling) between its vulva and its tails. For both assays, each worm was tested ten times and the number of times that trigger a reaction was assessed. Due to the fact that some of our strains appear lethargic we did not only consider forward movement as a reaction but any change in worm state occurring upon contact. To assess sensation of the nose, the eyelash was presented to the nose of the worm ten time and again all sign of detection were considered (backward movement or head bending). At least 30 worms over at least 3 different days were assessed for each test and strain.

Corpse assay

Predatory behaviour was tested as previously described with modifications (Eren et al., 2024; Wilecki et al., 2015). *C. elegans* larvae were collected from plates depleted in food just after hatching using M9 and passed through 20 µm filter to remove the other developmental stages. After centrifugation (2000 rpm, 1 min), ~1 µl of larvae was put off centre of a 6 cm unseeded plate, see supplementary figure 1A. In parallel, predators consisting of young adult *P. pacificus* of the strain of interest were picked onto another unseeded plates. Both predators and prey were left for 2 hours to allow the larval prey to spread and predator to starve. 5 predators were added on the plates and a copper arena 2.25 cm^2 was put around them. Assays was left for 2 hours then two pictures of the arena were taken at ~20x (each field covered a quarter of the arena) at least 10 second apart (Axio Zoom V16; Zeiss). The two images were process with Fiji using the 'max' set up and corpses were manually count on the resulting image. To assess kin recognition PS312 *P. pacificus* larvae were used as prey with 20 predator and the assay took place without the arena for 24 hours. Corpses were counted under the bench microscope (stemi 508, zeiss). For both assay 10 replicates were conducted at least three different days. To increase the power of our assay and detect smaller variation between strain, 20 replicas were made for figure 3.

Mouth form assessment

Worms were grown in OP50 plates until a high number of adults was reach. Worms were then washed in M9 and placed on a slide containing sodium azide to immobilized them. The number of eu and st worms were counted under an Axiovert 200 (zeiss) at 10x or 20x. Mouth form was controlled from 5 different plates over at least three different days with a minimum of 30 animals scored per assay.

Feeding assay with pharaglow

Pharaglow experiments were performed as described previously (Eren et al., 2024). Briefly, adult worms with a fluorescent pharynx marker (*Ppa-myo-2*p::RFP) were picked onto an unseeded plates and left for a 2 hour starvation period. 30 worms were picked onto unseeded assay plates containing *C. elegans* larvae made as for the killing assays (see above) but with twice the density to saturate the plate in larvae. To maintain the worms inside the field of view, a copper arena 2.25 cm^2 was put around the assay animals. Worms were acclimated to their new environment for 15 min before recording. Recording was made with an epi-fluorescence microscope (Axio Zoom V16, Zeiss) at 1x effective magnification (60 N-C ⅔'' 0.5 x, Zeiss) and Basler camera (acA3088-57um, BASLER). Light intensity was set at 100% and acquisition time was adjusted to use the full range of intensity without saturating the signal. Images were acquired at 30 Hz for 10 min. Images were then compressed and processed with the python package pharaglow (https://github.com/scholz-lab/PharaGlow), (Bonnard et al., 2022) adapted for *P. pacificus* (Eren et al., 2024) with the following parameters (subtract:1, smooth:3, dilate:3, tfactor:0.9, thresholdWindow:50, bgWindow:500, length:70, watershed:100, minSize:250, maxSize:1000, searchRange:10, memory:30, minimalDuration:1800, widthStraight:10, pad:5, nPts:50, linewidth:2). The quality of extracted movies was manually assessed and any worms with no sign of activity throughout the recording length were considered dead or damaged and removed from the analysis. Post-processing to calculate the velocity and pumping rate was done using a previously developed python script and finally automatic behavioural prediction were assigned using the git-hub package PpaPred as described previously (https://github.com/scholz-lab/PpaPred), (Eren et al., 2024). Worms were recorded over at least three different days. Total number of worms can be found in supplementary table 2.

Data representation and statistical analysis

Box plot illustrates data distribution with quartiles Q1, Q2, and Q3 representing the 25th, 50th, and 75th percentiles, respectively. The box, bounded by Q1 and Q3, includes a thicker line at the median (Q2). Whiskers show the range where most values fall. Analysis of chemosensory assay, touch assay, corpses assays and mouth form ratio was made with R software and its package prettyR with significance determine using one-direction Wilcoxon Mann Whitney with Benjamini-Hochberg correction (Lemon and Grosjean, 2019; R Core Team). Analysis of the state prediction results (relative time in state, mean bout duration, transition rates) were done with python has describe previously (Eren et al., 2024) relying on Wilcoxon Mann Whitney with Bonferroni correction and the precise p-value and sample size can be found in Supplementary table 2. In figures, statistics results is display as follow: non-significant (ns), p-value ≤ 0.05 (*), ≤ 0.01 (**), ≤ 0.001 (***), ≤ 0.0001 (****).

Acknowledgments

We would like to thank Wolfgang Bönigk for plasmid cloning (Genetics Facility, MPI for Neurobiology of Behavior-caesar), the Imaging facility for assistance (MPI for Neurobiology of Behavior-caesar) and Jürgen Berger for SEM imaging presented in figure 5 (MPI for Biology). The strains PS312 and RS3238 were provided by the Sommer lab (MPI for Biology, Tübingen).

Figure legends

Figure 1 *Ppa-mec-3* controls touch avoidance and prey detection.

(A) A *P. pacificus* adult predator (right) attacks a *C. elegans* larvae (left). Scale bar is 100 µm. (B) Representative image of a *P. pacificus* adult expressing *Ppa-mec-3p*::TurboRFP (top, magenta). Putative *P. pacificus* neuronal ID is based on *C. elegans* soma placement and known mechanosensory function. Scale bar is 100µm. (C) Mechanosensory assays to harsh touch, (D) gentle touch, and (E) nose touch. Each assessment is the result of ten consecutive trials of each worm. At least 30 worms were tested per strain. (F) Number of *C elegans* corpses counted after two hours of contact with the indicated *P. pacificus* strains as predator. At least 10 assays were performed. Statistical tests: one direction Wilcoxon Mann Whitney with Benjamini-Hochberg correction, non-significant (ns), p-value ≤ 0.05 (*), ≤ 0.01 (**), ≤ 0.001 (***), ≤ 0.0001 (****). Schematic were made with biorender.

Figure 2 Mechanosensation is involved in predation.

(A) Table analysing the number of mechanosensory gene paralogues compared to *C. elegans*. Species of free-living nematodes (brown), plant parasite nematodes (green) and animal parasite nematodes (black) are compared. Their evolutionary tree is presented on the left with the nematode clade marked. (B) Mechanosensory assays to harsh touch, (C) gentle touch, and (D) nose touch for *P. pacificus* mutants in putative mechanosensory genes. Each assessment is the result of ten consecutive trials of each worm. At least 30 worms were tested per strain. (E) Number of *C elegans* corpses counted after two hours of contact with the indicated *P. pacificus* putative mechanosensory mutants as predators. At least 10 assays were performed per mutant. Statistical tests: one direction Wilcoxon Mann Whitney with Benjamini-Hochberg correction, non-significant (ns), p-value ≤ 0.05 (*), ≤ 0.01 (**), ≤ 0.001 (***), ≤ 0.0001 (****). Schematic were made with biorender.

Figure 3: Chemosensation and mechanosensation synergically influence prey detection.

(A) Chemotaxis index analysing the aversive response of *Ppa-mec-3, Ppa-mec-6* and *Ppa-daf-19* to 1-octanol. Each genotype was assessed 10 time. (B) Percentage of *Ppa-mec-3, Ppa-mec-6* and *Ppa-daf-19* mutants finding a bacterial OP50 food source after 8 hours. Each genotype was assessed 10 time.
(C) Number of *C. elegans* corpses generated after two hours of exposure to the indicated *P. pacificus* mutants as predator. At least 20 assays were performed. Statistical results from comparison to wild-type (black) and to *daf-19* single mutant (green) are shown. Statistical tests: one direction Wilcoxon Mann Whitney with Benjamini-Hochberg correction, non-significant (ns), p-value ≤ 0.05 (*), ≤ 0.01 (**), ≤ 0.001 (***), ≤ 0.0001 (****). Schematic were made with biorender.

Figure 4: Behavioural tracking and analysis of sensory deficient worms in the presence of larvae.
(A) Schematic of behavioural tracking and machine learning workflow to track feeding behaviour and determine behavioural states based on a *Ppa-myo-2*::RFP pharyngeal fluorescence marker (established in Eren et al 2024). (B) Joint probability density map of velocity (μm/s) and pumping rate (Hz) for animals corresponding to the genotypes *Ppa-mec-6, Ppa-daf-19,* and *Ppa-mec-6; Ppa-daf-19.* The number of worms is indicated in the top right corner. (C) Time spent in each behavioral state normalized to the total track duration. Significance from comparison to wild-type (black) and to *daf-19* single mutant (green) was assessed using a Mann-Whitney U-test with a Bonferroni correction, non-significant (ns), p-value ≤ 0.05 (*), ≤ 0.01 (**), ≤ 0.001 (***), ≤ 0.0001 (****). Predatory (Pr.)

Figure 5: IL2 neurons are involved in prey detection
(A) Representative image of a worms expressing *Ppa-mec-6p*::Venus (top, green) and *Ppa-daf-19p*::TurboRFP (middle, magenta) and the merge (bottom). Scale bar is 100 μm. (B) Head of a worms expressing *mec-6p*::Venus (top, green) and *daf-19p*::TurboRFP (middle, magenta). Co-expression of both *Ppa-mec-6* and *Ppa-daf-19* visible in the merge image. Scale bar is 100 μm. (C) Scanning electron microscopy image of the anterior of a *P. pacificus* adults. The *P. pacificus* mouth opening is surrounded by protrusions of the 6 inner labial IL2 sensilla neurons. Scale bar is 3 μm (D) Putative model for the role and evolution of mechanosensation between *C. elegans* and *P. pacificus*. In both species, mechanosensation triggers an avoidance response which rely on *mec-3, mec-6, mec-4* and *mec-10.* In addition, in *P. pacificus,* contact can trigger predatory behaviour when the IL2 perceive mechanical or chemical stimuli. The perception of the predatory specific mechanical stimuli, acts through the mechanosensory pathway components *Ppa-mec-3* and *Ppa-mec-6.*

Fig sup1 mechanosensation and predation in *P.* pacificus

(A) Schematic of the corpse assay protocol. Five starved *P. pacificus* predators of the strain of interest are introduce in an area with an abundancy of *C. elegans* larvae. After 2 h, predatory success is assessed by counting the number of larval corpses inside the arena. In the image corpses can be observed inside the circles. Scale bar is 500 µm. (B) Mechanosensory assays to harsh touch, (C) gentle touch, and (D) nose touch. Each assessment is the result of ten consecutive trials of each worm. At least 30 worms were tested per strain. (E) Number of *C elegans* corpses counted after two hours of contact with the indicated *P. pacificus* strains as predator. At least 10 assays were performed. Statistical tests: one directionWilcoxon Mann Whitney with Benjamini-Hochberg correction, non-significant (ns), p-value ≤ 0.05 (*), ≤ 0.01 (**), ≤ 0.001 (***), ≤ 0.0001 (****). Schematic were made with biorender.

Fig sup2 mechanosensation does not affect developmental plasticity and kin-recognition

(A) *P. pacificus* can has a plastic development leading to two mouth form stenotomatous mouth (st, bottom) with the dorsal tooth (blue) or eurytomatous (eu, top) with an additional subventral tooth (red) and a wider opening. Scale bar is 10 µm. (B) Percentage of eu was assess 5 time for each strain. (C) Number of wild-type *P. pacificus* corpses counted after 24 hours of contact with the indicated *P. pacificus* strains as predator. Statistical tests: one directionWilcoxon Mann Whitney with Benjamini-Hochberg correction, non-significant (ns), p-value ≤ 0.05 (*), ≤ 0.01 (**), ≤ 0.001 (***), ≤ 0.0001 (****). Schematic were made with biorender.

Fig sup3 *Daf-19* muation affect the mouth form ratio but not touch detection

(A) Percentage of eu was assess 5 time for each strain. As shown in Moreno et al 2019, mutation of *Ppa-daf-19* lead to a higher occurrence of st mouth form which is prevented by mutation in *nag-1* and *nag-2*. *daf-19** is the only time mutation of *Ppa-daf*-19 is not studied in a strain also mutated for *nag-1* and *nag-2*. (B) Mechanosensory assays to harsh touch, (C) gentle touch, and (D) nose touch. Each assessment is the result of ten consecutive trials of each worm. At least 30 worms were tested per strain. Statistical tests: one direction Wilcoxon Mann Whitney with Benjamini-Hochberg correction, non-significant (ns), p-value ≤ 0.05 (*), ≤ 0.01 (**), ≤ 0.001 (***), ≤ 0.0001 (****). Schematic were made with biorender.

Fig sup4 Behavioural analysis of sensory deficient worms in the presence of prey.

(A) Joint probability density map of velocity (µm/s) and pumping rate (Hz) for animals corresponding to the indicated genotypes. The number of worms is indicated in the top right corner. (B) Time spent in each

behavioral state normalized to the total track duration. Statistical results from comparison to wild-type(black) and to *daf-19* single mutant (green) are shown. (C) Mean duration of each behaviour B. Statistical results from comparison to wild-type(black) and to *daf-19* single mutant (green) are shown. (D) Ethogram showing the predicted behaviour through time (X-axis) for each worm (Y-axis) for the indicated genotype. Statistical tests: Wilcoxon Mann Whitney with Bonferroni correction, non-significant (ns), p-value ≤ 0.05 (*), ≤ 0.01 (**), ≤ 0.001 (***), ≤ 0.0001 (****). Part of this figure use the same recording than in figure 4. Predatory (Pr.)

Reference:

Akduman, N., Rödelsperger, C. and Sommer, R. J. (2018). Culture-based analysis of Pristionchus-associated microbiota from beetles and figs for studying nematode-bacterial interactions. *PLoS One* **13**, e0198018.

Androwski, R. J., Asad, N., Wood, J. G., Hofer, A., Locke, S., Smith, C. M., Rose, B. and Schroeder, N. E. (2020). Mutually exclusive dendritic arbors in C. elegans neurons share a common architecture and convergent molecular cues. *PLOS Genetics* **16**, e1009029.

Athanasouli, M., Witte, H., Weiler, C., Loschko, T., Eberhardt, G., Sommer, R. J. and Rödelsperger, C. (2020). Comparative genomics and community curation further improve gene annotations in the nematode Pristionchus pacificus. *BMC Genomics* **21**, 708.

Auer, T. O., Khallaf, M. A., Silbering, A. F., Zappia, G., Ellis, K., Álvarez-Ocaña, R., Arguello, J. R., Hansson, B. S., Jefferis, G. S. X. E., Caron, S. J. C., et al. (2020). Olfactory receptor and circuit evolution promote host specialization. *Nature* **579**, 402–408.

Bargmann, C. I. (2006). Chemosensation in C. elegans. In *WormBook: The Online Review of C. elegans Biology [Internet]*, p. WormBook.

Baskaran, P., Rödelsperger, C., Prabh, N., Serobyan, V., Markov, G. V., Hirsekorn, A. and Dieterich, C. (2015). Ancient gene duplications have shaped developmental stage-specific expression in Pristionchus pacificus. *BMC Evol Biol* **15**, 185.

Bellono, N. W., Bayrer, J. R., Leitch, D. B., Castro, J., Zhang, C., O'Donnell, T. A., Brierley, S. M., Ingraham, H. A. and Julius, D. (2017). Enterochromaffin Cells Are Gut Chemosensors that Couple to Sensory Neural Pathways. *Cell* **170**, 185-198.e16.

Bento, G., Ogawa, A. and Sommer, R. J. (2010). Co-option of the hormone-signalling module dafachronic acid–DAF-12 in nematode evolution. *Nature* **466**, 494–497.

641 **Bianchi, L.** (2007). Mechanotransduction: Touch and Feel at the Molecular Level as Modeled in
642 Caenorhabditis elegans. *Mol Neurobiol* **36**, 254–271.

643 **Blaxter, M.** (2011). Nematodes: The Worm and Its Relatives. *PLOS Biology* **9**, e1001050.

644 **Blaxter, M. L., De Ley, P., Garey, J. R., Liu, L. X., Scheldeman, P., Vierstraete, A., Vanfleteren, J. R.,**
645 **Mackey, L. Y., Dorris, M., Frisse, L. M., et al.** (1998). A molecular evolutionary framework for the
646 phylum Nematoda. *Nature* **392**, 71–75.

647 **Bonnard, E., Liu, J., Zjacic, N., Alvarez, L. and Scholz, M.** (2022). Automatically tracking feeding behavior
648 in populations of foraging C. elegans. *Elife* **11**, e77252.

649 **Brown, A. L., Liao, Z. and Goodman, M. B.** (2008). MEC-2 and MEC-6 in the Caenorhabditis elegans
650 Sensory Mechanotransduction Complex: Auxiliary Subunits that Enable Channel Activity. *J Gen*
651 *Physiol* **131**, 605–616.

652 **Casasa, S., Katsougia, E. and Ragsdale, E. J.** (2023). A Mediator subunit imparts robustness to a
653 polyphenism decision. *Proc Natl Acad Sci U S A* **120**, e2308816120.

654 **Chalfie, M. and Sulston, J.** (1981). Developmental genetics of the mechanosensory neurons of
655 *Caenorhabditis elegans*. *Developmental Biology* **82**, 358–370.

656 **Chalfie, M. and Wolinsky, E.** (1990). The identification and suppression of inherited neurodegeneration
657 in Caenorhabditis elegans. *Nature* **345**, 410–416.

658 **Chalfie, M., Hart, A. C., Rankin, C. H. and Goodman, M. B.** (2014). Assaying mechanosensation.
659 *WormBook*.

660 **Chatzigeorgiou, M., Yoo, S., Watson, J. D., Lee, W.-H., Spencer, W. C., Kindt, K. S., Hwang, S. W., Miller,**
661 **D. M., Treinin, M., Driscoll, M., et al.** (2010). Specific roles for DEG/ENaC and TRP channels in
662 touch and thermosensation in C. elegans nociceptors. *Nat Neurosci* **13**, 861–868.

663 **Chelur, D. S., Ernstrom, G. G., Goodman, M. B., Yao, C. A., Chen, L., O' Hagan, R. and Chalfie, M.** (2002).
664 The mechanosensory protein MEC-6 is a subunit of the C. elegans touch-cell degenerin channel.
665 *Nature* **420**, 669–673.

666 **Chen, Y., Bharill, S., Altun, Z., O'Hagan, R., Coblitz, B., Isacoff, E. Y. and Chalfie, M.** (2016).
667 Caenorhabditis elegans paraoxonase-like proteins control the functional expression of
668 DEG/ENaC mechanosensory proteins. *Mol Biol Cell* **27**, 1272–1285.

669 **Choi, Y.-J., Ghedin, E., Berriman, M., McQuillan, J., Holroyd, N., Mayhew, G. F., Christensen, B. M. and**
670 **Michalski, M. L.** (2011). A Deep Sequencing Approach to Comparatively Analyze the
671 Transcriptome of Lifecycle Stages of the Filarial Worm, Brugia malayi. *PLOS Neglected Tropical*
672 *Diseases* **5**, e1409.

673 **Cook, S. J., Kalinski, C. A., Loer, C. M., Memar, N., Majeed, M., Stephen, S. R., Bumbarger, D. J.,**
674 **Riebesell, M., Schnabel, R., Sommer, R. J., et al.** (2024). Comparative connectomics of two
675 distantly related nematode species reveals patterns of nervous system evolution.
676 2024.06.13.598904.

677 **Cros, C. and Hobert, O.** (2022). Caenorhabditis elegans sine oculis/SIX-type homeobox genes act as
678 homeotic switches to define neuronal subtype identities. *Proceedings of the National Academy*
679 *of Sciences* **119**, e2206817119.

680 **Dardiry, M., Eberhard, G., Witte, H., Rödelsperger, C., Lightfoot, J. W. and Sommer, R. J.** (2023).
681 Divergent combinations of cis-regulatory elements control the evolution of phenotypic
682 plasticity. *PLoS Biol* **21**, e3002270.

683 **Dayi, M., Sun, S., Maeda, Y., Tanaka, R., Yoshida, A., Tsai, I. J. and Kikuchi, T.** (2020). Nearly Complete
684 Genome Assembly of the Pinewood Nematode Bursaphelenchus xylophilus Strain Ka4C1.
685 *Microbiol Resour Announc* **9**, e01002-20.

686 **De Stasio, E. A., Mueller, K. P., Bauer, R. J., Hurlburt, A. J., Bice, S. A., Scholtz, S. L., Phirke, P.,**
687 **Sugiaman-Trapman, D., Stinson, L. A., Olson, H. B., et al.** (2018). An Expanded Role for the RFX
688 Transcription Factor DAF-19, with Dual Functions in Ciliated and Nonciliated Neurons. *Genetics*
689 **208**, 1083–1097.

690 **Dutertre, S., Jin, A.-H., Vetter, I., Hamilton, B., Sunagar, K., Lavergne, V., Dutertre, V., Fry, B. G.,**
691 **Antunes, A., Venter, D. J., et al.** (2014). Evolution of separate predation- and defence-evoked
692 venoms in carnivorous cone snails. *Nat Commun* **5**, 3521.

693 **Emms, D. M. and Kelly, S.** (2019). OrthoFinder: phylogenetic orthology inference for comparative
694 genomics. *Genome Biology* **20**, 238.

695 **Eren, G. G., Roca, M., Han, Z. and Lightfoot, J. W.** (2022). Genomic integration of transgenes using UV
696 irradiation in Pristionchus pacificus. *MicroPubl Biol* **2022**,.

697 **Eren, G. G., Böger, L., Roca, M., Hiramatsu, F., Liu, J., Alvarez, L., Goetting, D., Zorn, N., Han, Z.,**
698 **Okumura, M., et al.** (2024). Predatory aggression evolved through adaptations to noradrenergic
699 circuits. 2024.08.02.606321.

700 **Flavell, S. W., Pokala, N., Macosko, E. Z., Albrecht, D. R., Larsch, J. and Bargmann, C. I.** (2013).
701 Serotonin and the neuropeptide PDF initiate and extend opposing behavioral states in C.
702 elegans. *Cell* **154**, 1023–1035.

703 **Foster, J., Ganatra, M., Kamal, I., Ware, J., Makarova, K., Ivanova, N., Bhattacharyya, A., Kapatral, V.,**
704 **Kumar, S., Posfai, J., et al.** (2005). The Wolbachia genome of Brugia malayi: endosymbiont
705 evolution within a human pathogenic nematode. *PLoS Biol* **3**, e121.

706 **Geffeney, S. L., Cueva, J. G., Glauser, D. A., Doll, J. C., Lee, T. H.-C., Montoya, M., Karania, S., Garakani,**
707 **A. M., Pruitt, B. L. and Goodman, M. B.** (2011). DEG/ENaC but Not TRP Channels Are the Major
708 Mechanoelectrical Transduction Channels in a C. elegans Nociceptor. *Neuron* **71**, 845–857.

709 **Goodman, M.** (2006). Mechanosensation. *WormBook*.

710 **Gracheva, E. O., Ingolia, N. T., Kelly, Y. M., Cordero-Morales, J. F., Hollopeter, G., Chesler, A. T.,**
711 **Sánchez, E. E., Perez, J. C., Weissman, J. S. and Julius, D.** (2010). Molecular basis of infrared
712 detection by snakes. *Nature* **464**, 1006–1011.

713 **Hall, R. P., Mutumi, G. L., Hedrick, B. P., Yohe, L. R., Sadier, A., Davies, K. T. J., Rossiter, S. J., Sears, K.,**
714 **Dávalos, L. M. and Dumont, E. R.** (2021). Find the food first: An omnivorous sensory
715 morphotype predates biomechanical specialization for plant based diets in phyllostomid bats*.
716 *Evolution* **75**, 2791–2801.

717 **Hammarlund, M., Hobert, O., Miller, D. M. and Sestan, N.** (2018). The CeNGEN Project: The Complete
718 Gene Expression Map of an Entire Nervous System. *Neuron* **99**, 430–433.

719 **Han, L., Wang, Y., Sangaletti, R., D'Urso, G., Lu, Y., Shaham, S. and Bianchi, L.** (2013). Two novel
720 DEG/ENaC channel subunits expressed in glia are needed for nose-touch sensitivity in
721 Caenorhabditis elegans. *J Neurosci* **33**, 936–949.

722 **Han, Z., Lo, W.-S., Lightfoot, J. W., Witte, H., Sun, S. and Sommer, R. J.** (2020). Improving Transgenesis
723 Efficiency and CRISPR-Associated Tools Through Codon Optimization and Native Intron Addition
724 in Pristionchus Nematodes. *Genetics* **216**, 947–956.

725 **Hart, A. C., Sims, S. and Kaplan, J. M.** (1995). Synaptic code for sensory modalities revealed by C.
726 elegans GLR-1 glutamate receptor. *Nature* **378**, 82–85.

727 **Hong, R. L. and Sommer, R. J.** (2006). Chemoattraction in *Pristionchus* Nematodes and Implications for
728 Insect Recognition. *Current Biology* **16**, 2359–2365.

729 **Hong, R. L., Witte, H. and Sommer, R. J.** (2008). Natural variation in Pristionchus pacificus insect
730 pheromone attraction involves the protein kinase EGL-4. *Proceedings of the National Academy*
731 *of Sciences* **105**, 7779–7784.

732 **Hunt, V. L., Tsai, I. J., Coghlan, A., Reid, A. J., Holroyd, N., Foth, B. J., Tracey, A., Cotton, J. A., Stanley,**
733 **E. J., Beasley, H., et al.** (2016). The genomic basis of parasitism in the Strongyloides clade of
734 nematodes. *Nat Genet* **48**, 299–307.

735 **Ishita, Y., Chihara, T. and Okumura, M.** (2021). Different combinations of serotonin receptors regulate
736 predatory and bacterial feeding behaviors in the nematode Pristionchus pacificus. *G3 (Bethesda)*
737 **11**, jkab011.

738 **Jiao, H., Xie, H.-W., Zhang, L., Zhuoma, N., Jiang, P. and Zhao, H.** (2021). Loss of sweet taste despite the
739 conservation of sweet receptor genes in insectivorous bats. *Proc Natl Acad Sci U S A* **118**,
740 e2021516118.

741 **Kalmijn, A. J.** (1971). The electric sense of sharks and rays. *J Exp Biol* **55**, 371–383.

742 **Kalmijn, A. J.** (1982). Electric and magnetic field detection in elasmobranch fishes. *Science* **218**, 916–918.

743 **Kindt, K. S., Viswanath, V., Macpherson, L., Quast, K., Hu, H., Patapoutian, A. and Schafer, W. R.**
744 (2007). Caenorhabditis elegans TRPA-1 functions in mechanosensation. *Nat Neurosci* **10**, 568–
745 577.

746 **Korhonen, P. K., Pozio, E., La Rosa, G., Chang, B. C. H., Koehler, A. V., Hoberg, E. P., Boag, P. R., Tan, P.,**
747 **Jex, A. R., Hofmann, A., et al.** (2016). Phylogenomic and biogeographic reconstruction of the
748 Trichinella complex. *Nat Commun* **7**, 10513.

Krochmal, A. R., Bakken, G. S. and LaDuc, T. J. (2004). Heat in evolution's kitchen: evolutionary perspectives on the functions and origin of the facial pit of pitvipers (Viperidae: Crotalinae). *J Exp Biol* **207**, 4231–4238.

Lee, H., Choi, M., Lee, D., Kim, H., Hwang, H., Kim, H., Park, S., Paik, Y. and Lee, J. (2011). Nictation, a dispersal behavior of the nematode Caenorhabditis elegans, is regulated by IL2 neurons. *Nat Neurosci* **15**, 107–112.

Lemon, J. and Grosjean, P. (2019). prettyR: Pretty Descriptive Stats.

Lightfoot, J. W., Wilecki, M., Rödelsperger, C., Moreno, E., Susoy, V., Witte, H. and Sommer, R. J. (2019). Small peptide-mediated self-recognition prevents cannibalism in predatory nematodes. *Science* **364**, 86–89.

Lightfoot, J. W., Dardiry, M., Kalirad, A., Giaimo, S., Eberhardt, G., Witte, H., Wilecki, M., Rödelsperger, C., Traulsen, A. and Sommer, R. J. (2021). Sex or cannibalism: Polyphenism and kin recognition control social action strategies in nematodes. *Sci Adv* **7**, eabg8042.

Liska, D., Wolfe, Z. and Norris, A. (2023). VISTA: Visualizing the Spatial Transcriptome of the C. elegans Nervous System. *bioRxiv* 2023.04.28.538711.

Lo, W.-S., Roca, M., Dardiry, M., Mackie, M., Eberhardt, G., Witte, H., Hong, R., Sommer, R. J. and Lightfoot, J. W. (2022). Evolution and Diversity of TGF-β Pathways are Linked with Novel Developmental and Behavioral Traits. *Mol Biol Evol* **39**, msac252.

McBride, C. S., Baier, F., Omondi, A. B., Spitzer, S. A., Lutomiah, J., Sang, R., Ignell, R. and Vosshall, L. B. (2014). Evolution of mosquito preference for humans linked to an odorant receptor. *Nature* **515**, 222–227.

Millet, J. R. M., Romero, L. O., Lee, J., Bell, B. and Vásquez, V. (2022). C. elegans PEZO-1 is a mechanosensitive ion channel involved in food sensation. *J Gen Physiol* **154**, e202112960.

Moreno, E., Lenuzzi, M., Rödelsperger, C., Prabh, N., Witte, H., Roeseler, W., Riebesell, M. and Sommer, R. J. (2018). DAF-19/RFX controls ciliogenesis and influences oxygen-induced social behaviors in Pristionchus pacificus. *Evol Dev* **20**, 233–243.

Moreno, E., Lightfoot, J. W., Lenuzzi, M. and Sommer, R. J. (2019). Cilia drive developmental plasticity and are essential for efficient prey detection in predatory nematodes. *Proc Biol Sci* **286**, 20191089.

Murray, R. W. (1960). Electrical Sensitivity of the Ampullæ of Lorenzini. *Nature* **187**, 957–957.

Musilova, Z., Cortesi, F., Matschiner, M., Davies, W. I. L., Patel, J. S., Stieb, S. M., de Busserolles, F., Malmstrøm, M., Tørresen, O. K., Brown, C. J., et al. (2019). Vision using multiple distinct rod opsins in deep-sea fishes. *Science* **364**, 588–592.

Nagai, T., Ibata, K., Park, E. S., Kubota, M., Mikoshiba, K. and Miyawaki, A. (2002). A variant of yellow fluorescent protein with fast and efficient maturation for cell-biological applications. *Nat Biotechnol* **20**, 87–90.

785 **Nakayama, K., Ishita, Y., Chihara, T. and Okumura, M.** (2020). Screening for CRISPR/Cas9-induced
786 mutations using a co-injection marker in the nematode Pristionchus pacificus. *Dev Genes Evol*
787 **230**, 257–264.

788 **Okumura, M., Wilecki, M. and Sommer, R. J.** (2017). Serotonin Drives Predatory Feeding Behavior via
789 Synchronous Feeding Rhythms in the Nematode Pristionchus pacificus. *G3 (Bethesda)* **7**, 3745–
790 3755.

791 **Olivera, B. M., Seger, J., Horvath, M. P. and Fedosov, A.** (2015). Prey-capture Strategies of Fish-hunting
792 Cone Snails: Behavior, Neurobiology and Evolution. *Brain Behav Evol* **86**, 58–74.

793 **Oteiza, P. and Baldwin, M. W.** (2021). Evolution of sensory systems. *Current Opinion in Neurobiology* **71**,
794 52–59.

795 **Perkins, L. A., Hedgecock, E. M., Thomson, J. N. and Culotti, J. G.** (1986). Mutant sensory cilia in the
796 nematode *Caenorhabditis elegans*. *Developmental Biology* **117**, 456–487.

797 **Prabh, N., Roeseler, W., Witte, H., Eberhardt, G., Sommer, R. J. and Rödelsperger, C.** (2018). Deep
798 taxon sampling reveals the evolutionary dynamics of novel gene families in Pristionchus
799 nematodes. *Genome Res* **28**, 1664–1674.

800 **Prieto-Godino, L. L., Rytz, R., Cruchet, S., Bargeton, B., Abuin, L., Silbering, A. F., Ruta, V., Dal Peraro,**
801 **M. and Benton, R.** (2017). Evolution of Acid-Sensing Olfactory Circuits in Drosophilids. *Neuron*
802 **93**, 661-676.e6.

803 **Procko, C., Murthy, S., Keenan, W. T., Mousavi, S. A. R., Dabi, T., Coombs, A., Procko, E., Baird, L.,**
804 **Patapoutian, A. and Chory, J.** (2021). Stretch-activated ion channels identified in the touch-
805 sensitive structures of carnivorous Droseraceae plants. *Elife* **10**, e64250.

806 **Procko, C., Wong, W. M., Patel, J., Mousavi, S. A. R., Dabi, T., Duque, M., Baird, L., Chalasani, S. H. and**
807 **Chory, J.** (2023). Mutational analysis of mechanosensitive ion channels in the carnivorous Venus
808 flytrap plant. *Curr Biol* **33**, 3257-3264.e4.

809 **R Core Team** R: A language and environment for statistical computing.

810 **Rabinowitch, I., Laurent, P., Zhao, B., Walker, D., Beets, I., Schoofs, L., Bai, J., Schafer, W. R. and**
811 **Treinin, M.** (2016). Neuropeptide-Driven Cross-Modal Plasticity following Sensory Loss in
812 Caenorhabditis elegans. *PLOS Biology* **14**, e1002348.

813 **Ragsdale, E. J., Müller, M. R., Rödelsperger, C. and Sommer, R. J.** (2013). A developmental switch
814 coupled to the evolution of plasticity acts through a sulfatase. *Cell* **155**, 922–933.

815 **Rhoades, J. L., Nelson, J. C., Nwabudike, I., Yu, S. K., McLachlan, I. G., Madan, G. K., Abebe, E., Powers,**
816 **J. R., Colón-Ramos, D. A. and Flavell, S. W.** (2019). ASICs Mediate Food Responses in an Enteric
817 Serotonergic Neuron that Controls Foraging Behaviors. *Cell* **176**, 85-97.e14.

818 **Rödelsperger, C., Meyer, J. M., Prabh, N., Lanz, C., Bemm, F. and Sommer, R. J.** (2017). Single-Molecule
819 Sequencing Reveals the Chromosome-Scale Genomic Architecture of the Nematode Model
820 Organism Pristionchus pacificus. *Cell Rep* **21**, 834–844.

821 **Salisbury, S. M., Martin, G. G., Kier, W. M. and Schulz, J. R.** (2010). Venom kinematics during prey
822 capture in Conus: the biomechanics of a rapid injection system. *J Exp Biol* **213**, 673–682.

823 **Schiffer, P. H., Kroiher, M., Kraus, C., Koutsovoulos, G. D., Kumar, S., R Camps, J. I., Nsah, N. A.,**
824 **Stappert, D., Morris, K., Heger, P., et al.** (2013). The genome of Romanomermis culicivorax:
825 revealing fundamental changes in the core developmental genetic toolkit in Nematoda. *BMC*
826 *Genomics* **14**, 923.

827 **Schroeder, N. E., Androwski, R. J., Rashid, A., Lee, H., Lee, J. and Barr, M. M.** (2013). Dauer-specific
828 dendrite arborization in C. elegans is regulated by KPC-1/Furin. *Curr Biol* **23**, 1527–1535.

829 **Shreffler, W., Magardino, T., Shekdar, K. and Wolinsky, E.** (1995). The unc-8 and sup-40 genes regulate
830 ion channel function in Caenorhabditis elegans motorneurons. *Genetics* **139**, 1261–1272.

831 **Sieriebriennikov, B., Prabh, N., Dardiry, M., Witte, H., Röseler, W., Kieninger, M. R., Rödelsperger, C.**
832 **and Sommer, R. J.** (2018). A Developmental Switch Generating Phenotypic Plasticity Is Part of a
833 Conserved Multi-gene Locus. *Cell Rep* **23**, 2835-2843.e4.

834 **Sieriebriennikov, B., Sun, S., Lightfoot, J. W., Witte, H., Moreno, E., Rödelsperger, C. and Sommer, R. J.**
835 (2020). Conserved nuclear hormone receptors controlling a novel plastic trait target fast-
836 evolving genes expressed in a single cell. *PLoS Genet* **16**, e1008687.

837 **Singh, P., Selvarasu, K. and Ghosh-Roy, A.** (2024). Optimization of RNAi efficiency in PVD neuron of C.
838 elegans. *PLoS One* **19**, e0298766.

839 **Staum, M., Abraham, A.-C., Arbid, R., Birari, V. S., Dominitz, M. and Rabinowitch, I.** (2024). Behavioral
840 adjustment of C. elegans to mechanosensory loss requires intact mechanosensory neurons.
841 *PLOS Biology* **22**, e3002729.

842 **Sternberg, P. W., Van Auken, K., Wang, Q., Wright, A., Yook, K., Zarowiecki, M., Arnaboldi, V., Becerra,**
843 **A., Brown, S., Cain, S., et al.** (2024). WormBase 2024: status and transitioning to Alliance
844 infrastructure. *Genetics* **227**, iyae050.

845 **Stevens, M.** (2013). *Sensory Ecology, Behaviour, and Evolution*. OUP Oxford.

846 **Tanimoto, Y., Zheng, Y. G., Fei, X., Fujie, Y., Hashimoto, K. and Kimura, K. D.** (2016). In actio
847 optophysiological analyses reveal functional diversification of dopaminergic neurons in the
848 nematode C. elegans. *Sci Rep* **6**, 26297.

849 **Tao, L., Porto, D., Li, Z., Fechner, S., Lee, S. A., Goodman, M. B., Xu, X. Z. S., Lu, H. and Shen, K.** (2019).
850 Parallel Processing of Two Mechanosensory Modalities by a Single Neuron in C. elegans. *Dev Cell*
851 **51**, 617-631.e3.

852 **Toda, Y., Ko, M.-C., Liang, Q., Miller, E. T., Rico-Guevara, A., Nakagita, T., Sakakibara, A., Uemura, K.,**
853 **Sackton, T., Hayakawa, T., et al.** (2021). Early origin of sweet perception in the songbird
854 radiation. *Science* **373**, 226–231.

855 **van Giesen, L., Kilian, P. B., Allard, C. A. H. and Bellono, N. W.** (2020). Molecular basis of chemotactile
856 sensation in octopus. *Cell* **183**, 594-604.e14.

857 **Wada-Katsumata, A., Silverman, J. and Schal, C.** (2013). Changes in taste neurons support the
858 emergence of an adaptive behavior in cockroaches. *Science* **340**, 972–975.

859 **Wang, Y., Apicella, A., Lee, S.-K., Ezcurra, M., Slone, R. D., Goldmit, M., Schafer, W. R., Shaham, S.,**
860 **Driscoll, M. and Bianchi, L.** (2008). A glial DEG/ENaC channel functions with neuronal channel
861 DEG-1 to mediate specific sensory functions in C. elegans. *EMBO J* **27**, 2388–2399.

862 **Way, J. C. and Chalfie, M.** (1988). mec-3, a homeobox-containing gene that specifies differentiation of
863 the touch receptor neurons in C. elegans. *Cell* **54**, 5–16.

864 **Werner, M. S., Sieriebriennikov, B., Loschko, T., Namdeo, S., Lenuzzi, M., Dardiry, M., Renahan, T.,**
865 **Sharma, D. R. and Sommer, R. J.** (2017). Environmental influence on Pristionchus pacificus
866 mouth form through different culture methods. *Sci Rep* **7**, 7207.

867 **Werner, M. S., Sieriebriennikov, B., Prabh, N., Loschko, T., Lanz, C. and Sommer, R. J.** (2018). Young
868 genes have distinct gene structure, epigenetic profiles, and transcriptional regulation. *Genome*
869 *Res* **28**, 1675–1687.

870 **Werner, M. S., Loschko, T., King, T., Reich, S., Theska, T., Franz-Wachtel, M., Macek, B. and Sommer, R.**
871 **J.** (2023). Histone 4 lysine 5/12 acetylation enables developmental plasticity of Pristionchus
872 mouth form. *Nat Commun* **14**, 2095.

873 **Wilecki, M., Lightfoot, J. W., Susoy, V. and Sommer, R. J.** (2015). Predatory feeding behaviour in
874 Pristionchus nematodes is dependent on phenotypic plasticity and induced by serotonin. *J Exp*
875 *Biol* **218**, 1306–1313.

876 **Witte, H., Moreno, E., Rödelsperger, C., Kim, J., Kim, J.-S., Streit, A. and Sommer, R. J.** (2015). Gene
877 inactivation using the CRISPR/Cas9 system in the nematode Pristionchus pacificus. *Dev Genes*
878 *Evol* **225**, 55–62.

879 **Xiao, R. and Xu, X. Z. S.** (2009). Function and regulation of TRP family channels in C. elegans. *Pflugers*
880 *Archiv : European journal of physiology* **458**, 851.

881 **Zjacic, N. and Scholz, M.** (2022). The role of food odor in invertebrate foraging. *Genes Brain Behav* **21**,
882 e12793.

883

884

885

886

887
888

889

890

Figure 1

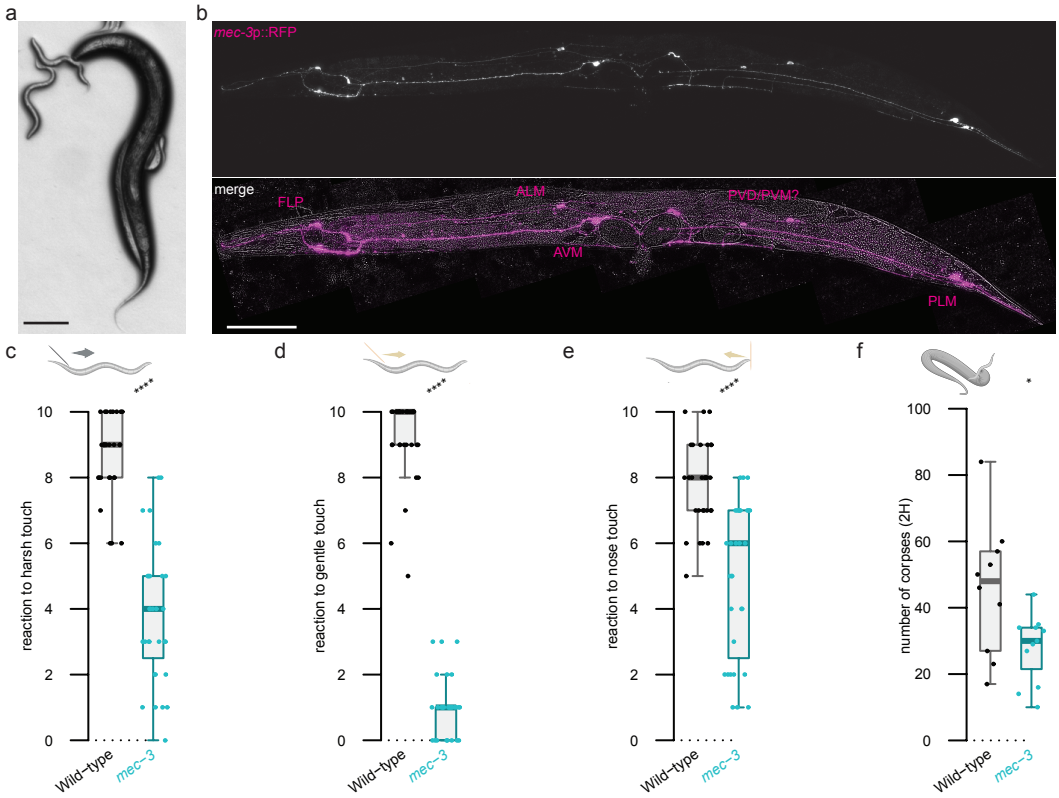
a
b
mec-3p::RFP
merge
FLP
ALM
PVD/PVM?
AVM
PLM
c
d
e
f
****
****
****
*
reaction to harsh touch
reaction to gentle touch
reaction to nose touch
number of corpses (2H)
0
2
4
6
8
10
0
20
40
60
80
100
Wild-type
mec-3

Figure 2

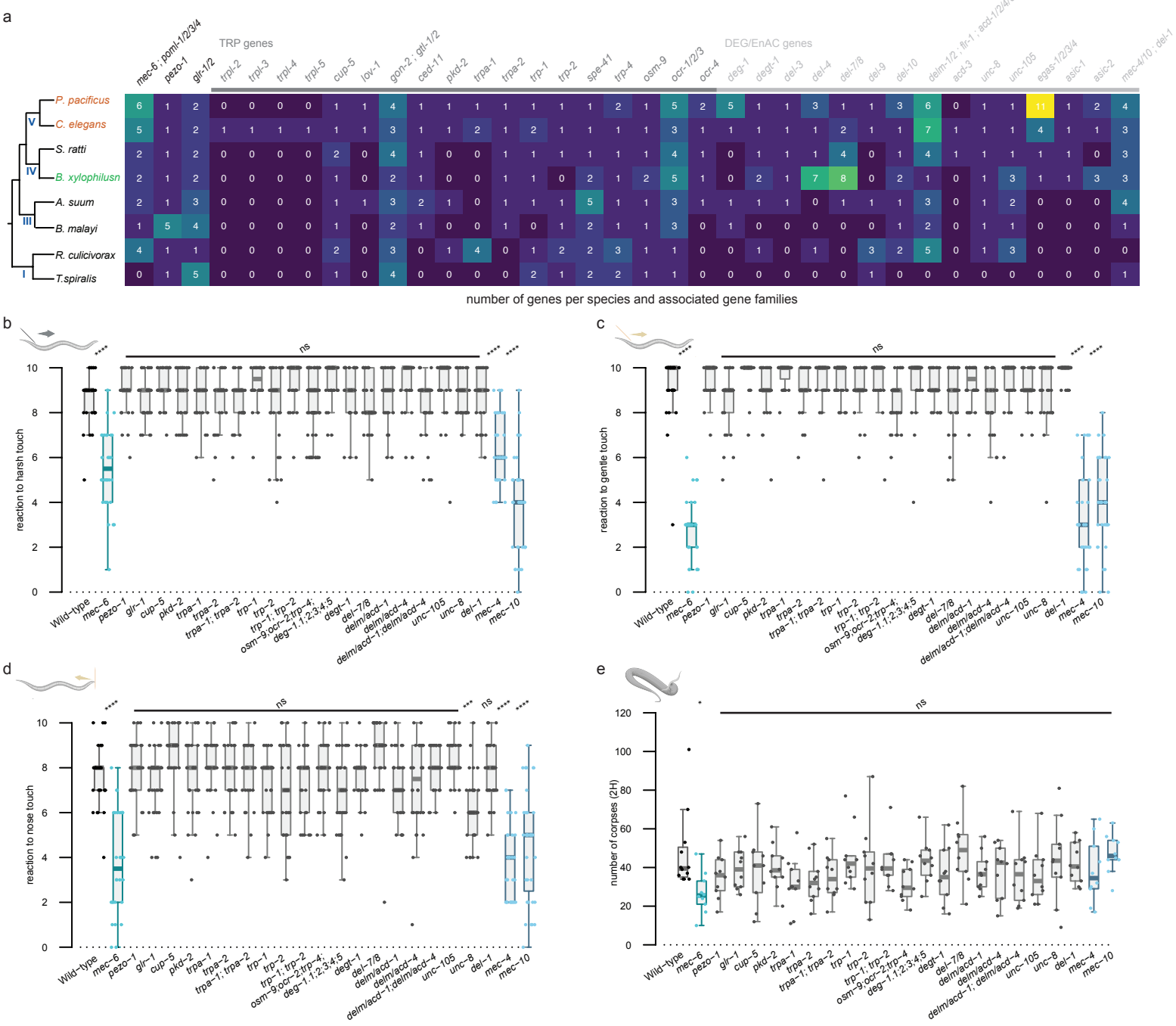
a
TRP genes
DEG/EnAC genes
mec-6 ; pomt-1/2/3/4
pezo-1
glr-1/2
trpl-2
trpl-3
trpl-4
trpl-5
cup-5
lov-1
gon-2 ; gtl-1/2
ced-11
pkd-2
trpa-1
trpa-2
trp-1
trp-2
spe-41
trp-4
osm-9
ocr-1/2/3
ocr-4
deg-1
degt-1
del-3
del-4
del-7/8
del-9
del-10
delm-1/2 ; flr-1 ; acd-1/2/4/5
acd-3
unc-8
unc-105
egas-1/2/3/4
asic-1
asic-2
mec-4/10 ; del-1
P. pacificus
C. elegans
S. ratti
B. xylophilusn
A. suum
B. malayi
R. culicivorax
T.spiralis
V
IV
III
I
number of genes per species and associated gene families
b
reaction to harsh touch
c
reaction to gentle touch
d
reaction to nose touch
e
number of corpses (2H)
ns
Wild-type
mec-6
pezo-1
glr-1
cup-5
pkd-2
trpa-1
trpa-2
trp-1
trp-2
trp-1; trp-2
osm-9;ocr-2;trp-4;
deg-1;2;3;4;5
degt-1
del-7/8
delm/acd-1
delm/acd-4
unc-105
unc-8
del-1
mec-4
mec-10

Figure 3

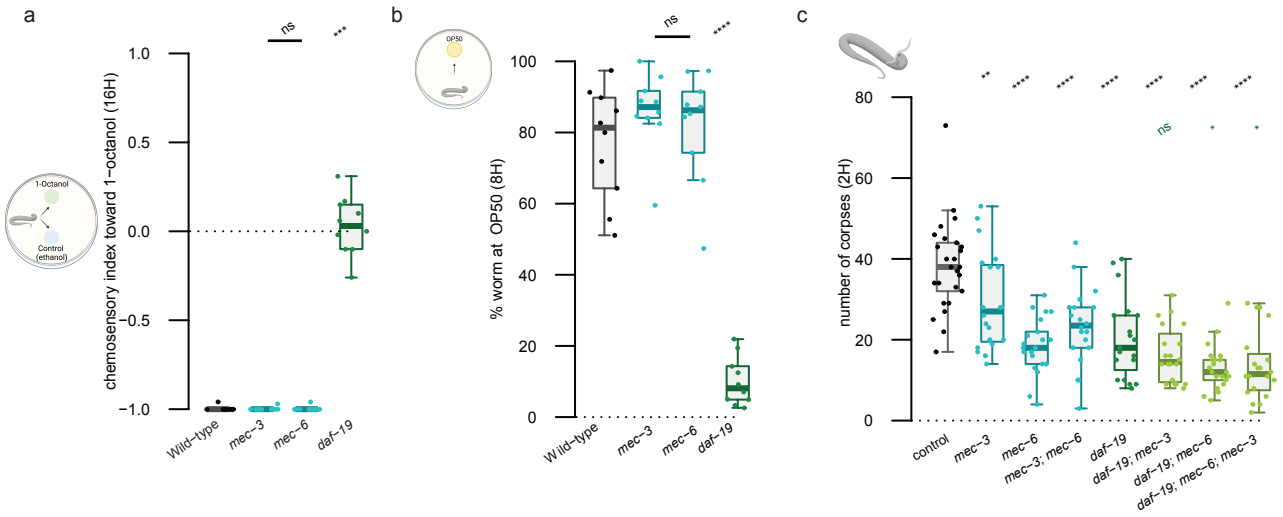
a
1-Octanol
Control (ethanol)
chemosensory index toward 1−octanol (16H)
1.0
0.5
0.0
−0.5
−1.0
ns
***
Wild−type
mec−3
mec−6
daf−19
b
OP50
% worm at OP50 (8H)
100
80
60
40
20
0
ns
****
Wild−type
mec−3
mec−6
daf−19
c
number of corpses (2H)
80
60
40
20
0
**
****
****
****
ns
****
*
*
control
mec−3
mec−6
mec−3; mec−6
daf−19
daf−19; mec−3
daf−19; mec−6
daf−19; mec−6; mec−3

Figure 4

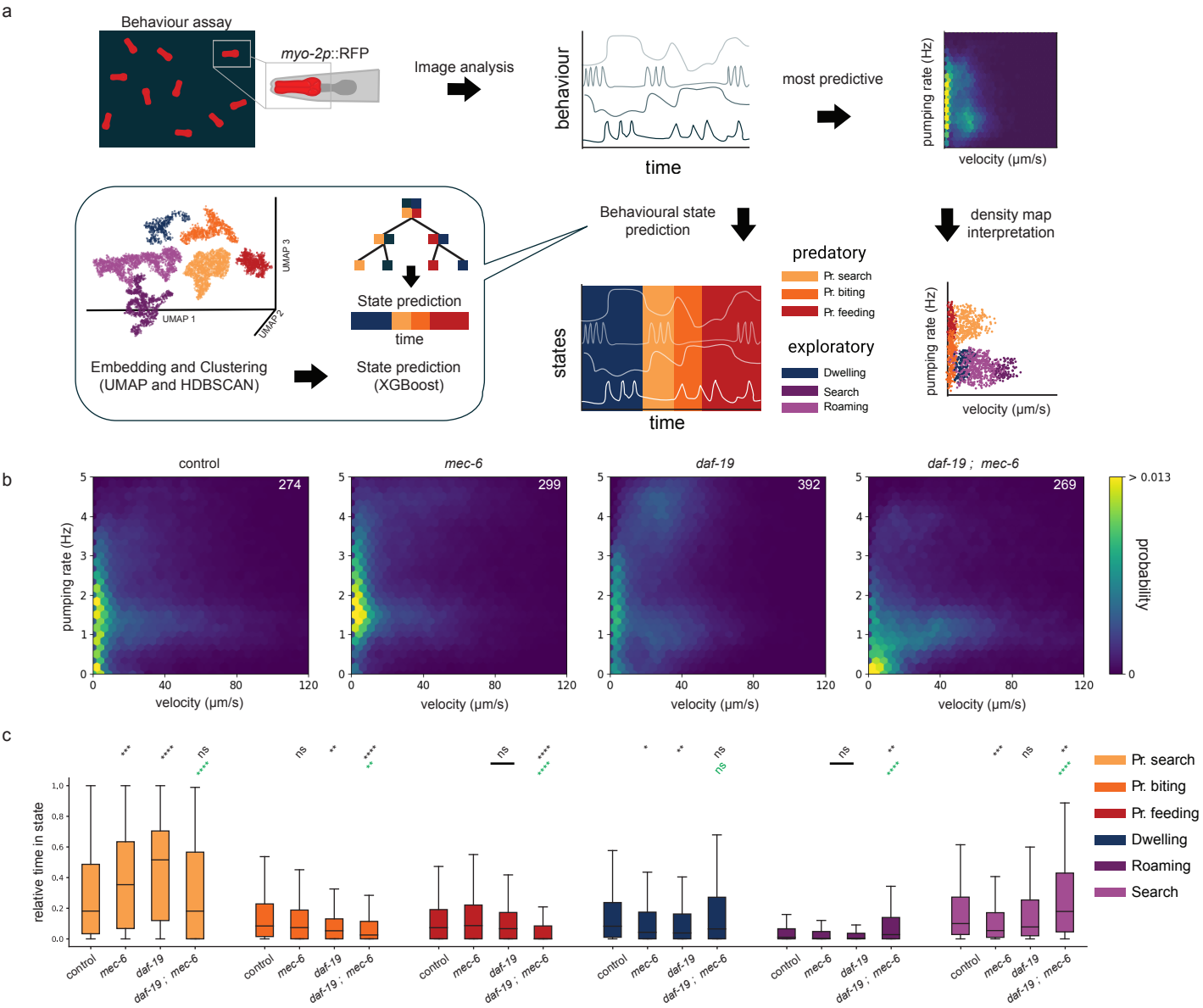
a
Behaviour assay
myo-2p::RFP
Image analysis
behaviour
time
most predictive
pumping rate (Hz)
velocity (µm/s)
UMAP 1
UMAP 2
UMAP 3
Embedding and Clustering
(UMAP and HDBSCAN)
State prediction
time
State prediction
(XGBoost)
Behavioural state
prediction
density map
interpretation
states
time
predatory
Pr. search
Pr. biting
Pr. feeding
exploratory
Dwelling
Search
Roaming
b
control
mec-6
daf-19
daf-19 ; mec-6
274
299
392
269
pumping rate (Hz)
velocity (µm/s)
> 0.013
probability
c
relative time in state
control
mec-6
daf-19
daf-19 ; mec-6
Pr. search
Pr. biting
Pr. feeding
Dwelling
Roaming
Search

Figure 5

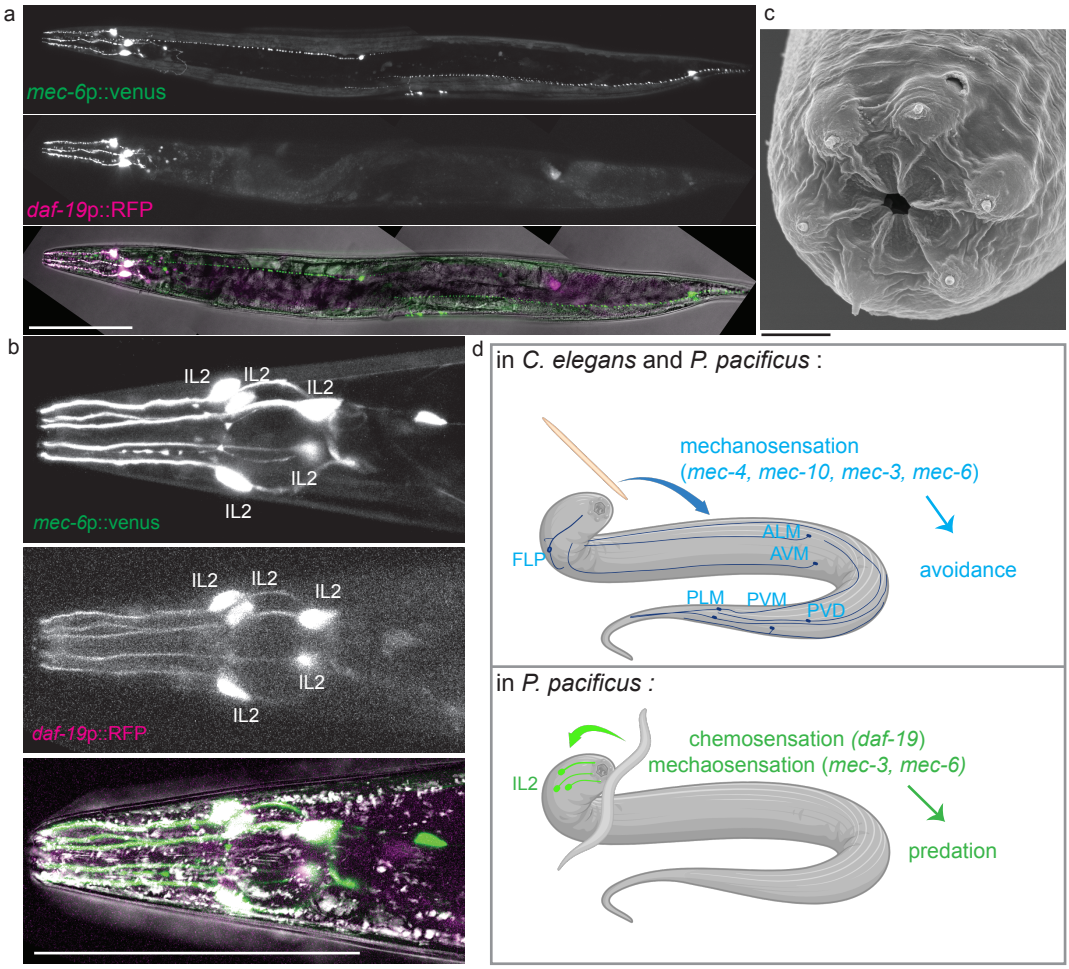
a
mec-6p::venus
daf-19p::RFP
c
b
IL2
IL2
IL2
IL2
IL2
mec-6p::venus
IL2
IL2
IL2
IL2
IL2
daf-19p::RFP
d
in C. elegans and P. pacificus :
mechanosensation
(mec-4, mec-10, mec-3, mec-6)
FLP
ALM
AVM
PLM
PVM
PVD
avoidance
in P. pacificus :
IL2
chemosensation (daf-19)
mechaosensation (mec-3, mec-6)
predation